Conical refraction output from a Nd:YVO₄ laser with an intracavity conerefringent element

R. Akbari[1], C. Howlader[1], K.A. Fedorova[2], G.S. Sokolovskii[3,4], E.U. Rafailov[5], and A. Major[1,*]

[1]Department of Electrical and Computer Engineering, University of Manitoba, Winnipeg, R3T 5V6, Canada
[2]Department of Physics, Philipps-Universität Marburg, Marburg, 35032, Germany
[3]Ioffe Institute, St. Petersburg, 194021, Russia
[4]Saint Petersburg Electrotechnical University (LETI), St. Petersburg, 197022, Russia
[5]School of Engineering & Applied Science, Aston University, Birmingham, B4 7ET, UK
*Corresponding author: a.major@umanitoba.ca

A conical refraction (CR) laser based on an a-cut Nd:YVO₄ laser was demonstrated. By using a KGW crystal as a CR element, a typical laser with a Gaussian intensity output profile was transformed into a laser with conically refracted output. The CR laser delivered 220 mW of output power for 500 mW of pump power. The separation of the laser gain medium and the CR element reduced the complexity of the pumping scheme and resulted in the generation of well-behaved CR laser beams with outstanding quality. The presented approach is power-scalable and offers a unique possibility of studying the transformation of a Gaussian laser mode into a conically refracted one in a laser cavity.

OCIS Codes: (140.3480) Lasers, diode-pumped; (140.3530) Lasers, neodymium; (140.3580) Lasers, solid-state; (120.5710) Refraction.

The intriguing phenomenon of conical refraction (CR) has attracted a lot of attention in recent years due to its fundamental properties and practical applications, which were thoroughly reviewed in Ref. [1]. A common picture is that in a biaxial crystal, a conically refracted beam with a Gaussian intensity profile transforms into a characteristic pair of bright concentric rings separated by a dark Poggendorff ring. The polarization of the concentric ring pattern in the focal (Lloyd) plane is another signature of CR and is such that any two diametrically opposite points on the ring have orthogonal polarizations. In addition, the propagation of the CR beam is symmetric with respect to the Lloyd plane and its axial evolution away from it produces a bright central (Raman) spot in the far field. While theoretical studies have established a firm understanding of the formation and properties of the "passive" CR beams [1–8], the area of CR lasers is relatively new with only a few reports [9–14]. In CR lasers, the gain medium also functions as a CR element, therefore producing a complex relationship between the classical effect of CR, anisotropic laser gain, as well as resonant conditions of the optical cavity. As a consequence, the effect of CR on a Gaussian laser mode in the cavity is still not well understood. For example, in some cases a laser beam with a Gaussian intensity output profile was produced after the plane output mirror [11,13], whereas in the other experiments the output beam had a crescent-like shape [12,14], only resembling the CR beam. Moreover, in none of the previous CR laser experiments a clear concentric double-ring pattern (i.e. with a dark Poggendorff ring) was observed making it difficult, if not impossible, to accurately study the actual beam transformation inside and its evolution outside of the laser cavity.

In this work we propose and demonstrate a simple solution to reduce the complexity of the "active" CR, where the laser gain medium also acts as a CR element, by decoupling the gain and CR media. This is done by using a laser with a separate intracavity conerefringent element (CRE). There are numerous advantages of this approach: 1) a Gaussian laser mode in the resonator interacts with a separate CRE which facilitates laser adjustment for the CR beam generation; 2) optimal laser gain and CR conditions can be achieved more independently; 3) the laser properties (e.g. wavelength) are not limited by the properties of the CRE host material; 4) separate laser gain medium also allows power scaling. This proof-of-principle work was based on a Nd:YVO₄ laser with an intracavity CRE formed by the biaxial crystal of KGW (KGd(WO₄)₂). As a result of its advantages, the proposed setup produced images of the CR laser beams of unprecedented quality. Different CR beam generation regimes were also studied and one of the main CR laser beam forming conditions was identified and experimentally confirmed.

In our experiments, a crystal of Nd:YVO₄ was used as a laser gain medium. It is a uniaxial crystal from the vanadate family that is well-known for its highly polarized emission and efficient operation in the continuous-wave [15–17] and pulsed [18,19] regimes. The laser employed a 3 mm-long a-cut 1.1 at. % Nd:YVO₄

crystal in a five-mirror cavity configuration as shown in Fig. 1(a). The crystal had anti-reflective (AR) coating for 808 nm and 1064 nm on both surfaces. The crystal was wrapped in indium foil and placed in a heat sink. The pumping system consisted of a home-built Ti:sapphire laser with the oscillating wavelength tuned to 808.8 nm by means of a 0.5 mm-thick birefringent filter. The pump beam was focused in the laser crystal into a spot size with a diameter of 35 μm. A maximum incident pump power of 500 mW was available for the experiments. The mirror R3 provided a suitable focusing of the laser mode into the CRE.
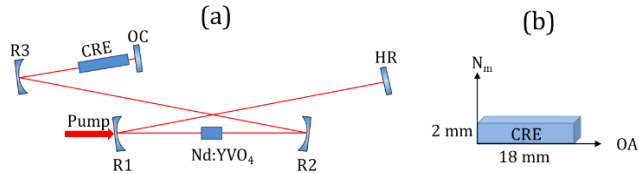

Fig. 1. (a) Schematic of the laser cavity. R1 = R2 = −100 mm, R3 = −150 mm. OC: output coupler, HR: highly reflective mirror, CRE: conerefringent element. (b) Schematic of the CRE (KGW crystal), OA: optical axis.

The laser was firstly operated without the CRE in the cavity and produced a horizontally polarized high quality output beam with a Gaussian intensity profile at 1064.35 nm. By using a 5% output coupling mirror, the laser delivered >300 mW of output power at 500 mW of pump power. In order to study the CR laser output, an 18 mm-long AR-coated KGW crystal (i.e. CRE) cut along its optical axis (see Fig. 1(b)) was introduced into the cavity close to the output coupler (OC). The KGW crystal is a typical choice for the active/passive CR experiments and applications [9,11–14,20–23]. This crystal is characterized by strong anisotropy of its optical and physical parameters [24,25] as well as good optical quality that made it a popular host for rare-earth metal ion based lasers [14,26–29]. The CRE was oriented such that its N_m-axis was horizontal. The separation of the R3-OC mirrors was correspondingly adjusted to retain the stability of the laser cavity. The output beam from the laser was monitored using an imaging lens (f = 60 mm) and a digital camera. The position of the image plane was approximately 3-5 mm outside of the output coupler. For large misalignment between the directions of the optical axis of the CRE and the laser mode axis, the laser delivered negligible output power. By further adjustment of the CRE, the laser could operate in double refraction regime with two distinct spots (or one spot and a crescent) in the output beam with an increased output power. Approaching the parallel direction of the optical axis of the KGW crystal with respect to the laser mode axis, the ring-shaped patterns in the laser output could be observed. A precise adjustment of the CRE together with the output coupler was required in order to obtain a fully resolved CR beam with a dark Poggendorff ring. In this particular case, a ring-shaped CR output laser beam with a dark area (i.e. node) at the bottom of the ring was achieved, which is the characteristic of a conically refracted linearly polarized laser beam with a Gaussian intensity profile (see Fig. 2 (a)) [1]. We believe that the images of the CR laser beam of such a high quality were produced for the first time. In this regime (with the 5% output coupler) the laser delivered 220 mW of output power for the pump power of 500 mW. Similar to the well-known free-space CR beam propagation [1], the generated laser beam exhibited the same evolution pattern along its propagation axis away from the Lloyd image plane towards the Raman spot (see Fig. 2 (a)-(d)). To further confirm the CR nature of the obtained radiation, the polarization distribution along the CR beam ring pattern was analyzed using a rotating polarizer (see Fig. 2 (e)). A laser with CR output was also realized for the orthogonal orientation of the CRE (i.e. vertical orientation of the N_m-axis). In this case the node of the CR beam and the distribution of the polarization states along the ring rotated by 90 degrees (see figures (f)-(j)).
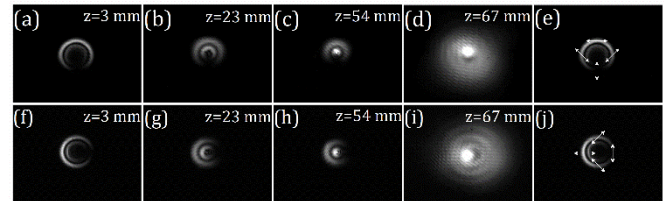

Fig. 2. The CR laser beam at the Lloyd image plane and its free-space evolution for the CRE with horizontal orientation of the N_m-axis (a)-(d) and vertical orientation of the N_m-axis (f)-(i). The local polarization states of the CR beams were determined by a polarizer and are marked by arrows in (e) and (j). The far-field beams in (d) and (i) were imaged without an imaging lens. The numbers show the positions of the image planes calculated/measured from the outer surface of the output coupler.

In order to evaluate the performance of the CR laser against an equivalent non-CR laser (i.e. a typical laser with a Gaussian beam intensity profile), a 20 mm-long AR-coated N_g-cut (non-CR) KGW crystal was inserted instead of the CRE in the cavity. The laser produced an output beam with transverse intensity distribution of a fundamental Gaussian mode and with higher maximum output power of 287 mW (for 500 mW of incident pump power). The slope efficiency of the laser was 58%, while the CR laser could generate the maximum output power of 220 mW with the slope efficiency of 44%. In Fig. 3 the performance of the CR laser was compared with the non-CR lasers with and without the non-CR crystal.
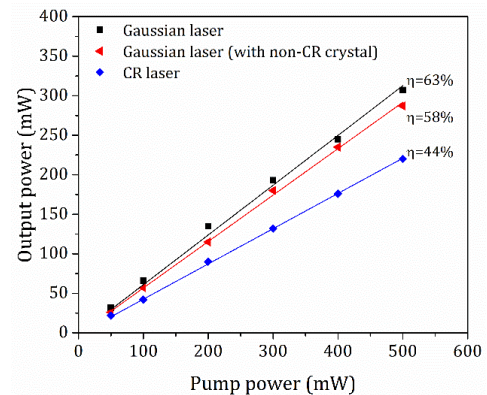

Fig. 3. The output powers vs. pump power for the free-running non-CR laser (with and without the non-CR crystal) as well as for the CR laser.

Another feature of the CR beams is that the formation of the CR pattern is strongly affected by the ratio of the CR ring and the input beam radii $\rho_0 = R_0/\omega_0$. The formation of a clear CR pattern requires $\rho_0 >> 1$ [8]. While described in detail in the theoretical works [1,7,8], this condition was overlooked in the previous CR laser reports. In analogy with the passive CR beams, the thickness of concentric

rings of the produced CR beam pattern and the pattern itself should depend on the laser mode size incident on the intracavity CRE. Since the mode size is controlled by the radius of curvature (ROC) of the focusing mirror R3 (see Fig. 1(a)), this effect was investigated using focusing mirrors with different values of ROC. Using a mirror with ROC = −100 mm, a finer ring pattern of the CR beam could be generated, while increasing the ROC of the focusing mirror resulted in wider rings as expected (see Fig. 4). For an intermediate value of ROC = −300 mm the inner ring collapsed to a central spot (Fig. 4(d)) and for a sufficiently large value of ROC = −750 mm the CR beam resembled a crescent-like pattern (Fig. 4(f)) that was actually observed in the previous CR laser reports [10,12–14]. This observation sheds light on previous CR laser results and experimentally confirms one of the main CR laser beam forming conditions in a laser cavity. At the same time, it should be mentioned that the respective CR laser output power increased from 190 mW to 260 mW by increasing the ROC from −100 mm to −500 mm. However, the output power decreased to 210 mW for the largest ROC of −750 mm. The reduction in output power in this case probably can be attributed to a mismatch between the CR laser mode and the pump beam in the laser crystal.
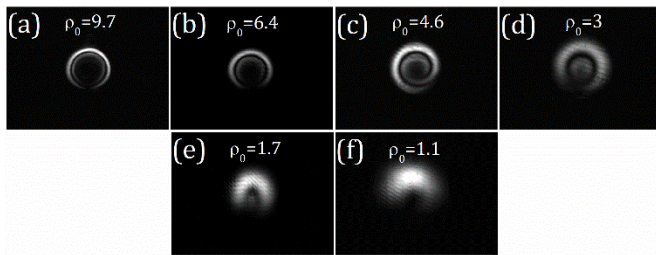

Fig. 4. The CR laser beams for different ROCs of the focusing mirror R3. (a) R3 = −100 mm, P_{out} = 190 mW, (b) R3 = −150 mm, P_{out} = 220 mW, (c) R3 = −200 mm, P_{out} = 233 mW, (d) R3 = −300 mm, P_{out} = 250 mW, (e) R3 = −500 mm, P_{out} = 260 mW, (f) R3 = −750 mm, P_{out} = 210 mW. The numbers show the estimated ratio ρ_0 of the CR ring radius (R_0) to the Gaussian laser mode waist radius (in our case R_0 = 306 μm). For all cases the position of the image plane was similar. The observed patterns have very good agreement with theoretical results in Ref. [1].

In order to examine the effect of the ROC of the output coupler on the CR laser, a curved HR mirror (ROC = −500 mm) was used instead of the flat output coupler. In this case the HR mirror in the opposite arm was replaced by the 5% output coupler and the focusing R3 mirror had −150 mm of ROC. The CR laser mode behind the curved HR end mirror was observed by the camera. The laser delivered a lower output power (175 mW) and the CR beam (behind the curved HR mirror) with reduced sharpness and resolvability when compared to the original cavity with the flat output coupler.

The separation of the laser gain medium and the CRE in the cavity made it possible to conveniently extend a laser with a Gaussian intensity output profile to a CR laser and generate a well-characterized CR beam. In previous works on the CR lasers, the CREs were employed as the laser gain medium and the laser cavity configurations and pumping schemes were limited by the conically refracted laser mode in the laser crystal [10–14].

The performance of the CR laser in terms of output power showed its reduction when compared to the equivalent non-CR lasers with and without the non-CR KGW crystal in the cavity (see

Fig. 3). We believe that this can be explained by different spatial profiles of the resonating modes of the CR and non-CR lasers. Given the pump spot size diameter in the crystal of only 35 μm, even a small deviation in the size of the resulting CR cavity mode can have a sizeable effect on the overlap with the pumped area and lead to the reduction in output power.

In order to investigate the laser mode evolution in the cavity, the leakage from the flat HR mirror in the opposite cavity arm (see Fig. 5(a)) was also imaged. This produced an "HR beam". The beam profiles of the laser outputs from the HR arms of the CR laser and the non-CR laser are shown in Fig. 5 (a) and (b), respectively. It can be seen that the CR laser mode (Fig. 5(a)) is similar to the Raman spot of the CR beam. There is a noticeable concentric intensity background around it, which is absent in the case of a Gaussian laser mode (Fig. 5(b)). This clearly points to the mode shaping induced by the intracavity CRE that can result in less than optimal overlap of the CR mode with the pumped area in the Nd:YVO$_4$ crystal.

Furthermore, the CRE cavity arm was folded using an additional (low transmission) flat output coupler OC2 (see Fig.5 (a)). The OC2 was located between the R2 and R3 mirrors and therefore produced two auxiliary output beams: one that was going towards the CRE after the double-pass of the laser crystal (beam 1) and another one that was going towards the laser crystal after the double-pass of the CRE (beam 2). In the CR laser regime, the laser modes at the place of OC2 (beams 1 and 2) exhibited more sophisticated behavior. As shown in Fig. 5, although the CR laser cavity mode coming towards the CRE (beam 1) exhibited a Gaussian-like intensity distribution (Fig. 5(c)), the laser mode after the double-pass through the CRE (beam 2) had a much more complex intensity distribution (Fig. 5(d)).
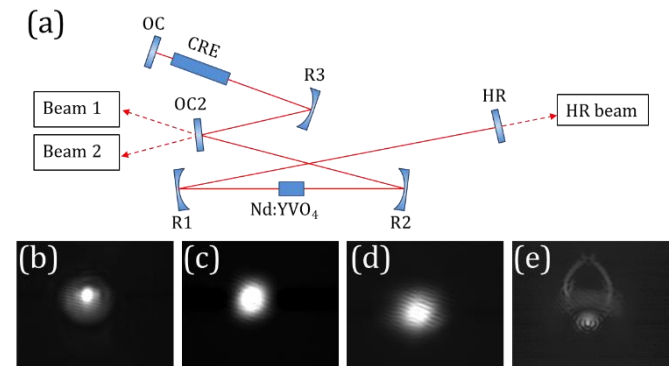

Fig. 5. (a) Schematic of the modified CR laser cavity for observation of the intermediate laser mode shapes. Intensity profiles of the laser output beams from the HR arms for the (b) CR and (c) typical non-CR lasers. Intensity profiles of the auxiliary laser output beams (produced by the additional flat OC2) corresponding to the intracavity beams coming (d) towards the CRE (beam 1, double-pass through the Nd:YVO$_4$) and (e) towards the laser crystal (beam 2, double-pass through the CRE). The image in (e) shows a larger area than in (b-d) in order to include all beam shape details.

We believe that this drastic transformation of the laser mode in the CR cavity and its spatial mismatch with the pump beam accounted for the reduction in the output power when compared to the laser with a Gaussian intensity output profile. At the same time, it is interesting to note that the laser mode regained its Gaussian-like intensity profile (see Fig. 5(c)) and polarization after its second

passage through the gain medium. These observations require further experimental and numerical studies on the CR cavity mode formation in order to fully understand this process and, for example, optimize the laser mode matching with the pump beam.

In conclusion, a CR laser that used the separate gain and CR media was demonstrated. This enabled the laser to produce a well-behaved CR laser beam with excellent quality. The CR laser was based on an a-cut Nd:YVO$_4$ laser and an intracavity KGW crystal as a CRE. The laser produced up to 220 mW of average output power with a well-resolved CR beam while intracavity power reached 4.4 W. It was experimentally shown that the laser mode focusing conditions play an important role in the formation of a CR beam pattern. The performance of the CR laser was compared to the standard laser with a Gaussian intensity output profile and was found to be affected by the intracavity CR mode transformation [30] leading to a slight reduction in the output power. Owing to the separation of the laser gain crystal and the CRE, the laser has the potential for power scaling using the efficient diode pumping approach [16,18] as well as increased flexibility in laser operating parameters such as, for example, wavelength [31,32]. We believe that the results of this work will contribute to further development of theory and practice of the CR lasers and resonators.

References

1. A. Turpin, Y. V. Loiko, T. K. Kalkandjiev, and J. Mompart, Laser Photon. Rev. **10**, 750–771 (2016).
2. A. M. Belsky and A. P. Khapalyuk, Opt. Spectrosc. **44**, 436 (1978).
3. A. M. Belsky and M. A. Stepanov, Opt. Commun. **167**, 1–5 (1999).
4. M. V. Berry, J. Opt. A Pure Appl. Opt. **6**, 289–300 (2004).
5. C. F. Phelan, K. E. Ballantine, P. R. Eastham, J. F. Donegan, and J. G. Lunney, Opt. Express **20**, 13201 (2012).
6. G. S. Sokolovskii, D. J. Carnegie, T. K. Kalkandjiev, and E. U. Rafailov, Opt. Express **21**, 11125 (2013).
7. A. Turpin, Y. V. Loiko, T. K. Kalkandkiev, H. Tomizawa, and J. Mompart, Opt. Lett. **39**, 4349 (2014).
8. M. V. Berry, M. R. Jeffrey, and J. G. Lunney, Proc. R. Soc. A Math. Phys. Eng. Sci. **462**, 1629–1642 (2006).
9. J. Hellström, H. Henricsson, V. Pasiskevicius, U. Bünting, and D. Haussmann, Opt. Lett. **32**, 2783 (2007).
10. A. Brenier, Laser Phys. **27**, 105001 (2017).
11. A. Abdolvand, K. G. Wilcox, T. K. Kalkandjiev, and E. U. Rafailov, Opt. Express **18**, 2753 (2010).
12. A. Brenier, Appl. Phys. B **122**, 237 (2016).
13. K. G. Wilcox, A. Abdolvand, T. K. Kalkandjiev, and E. U. Rafailov, Appl. Phys. B **99**, 619–622 (2010).
14. R. Cattoor, I. Manek-Hönninger, D. Rytz, L. Canioni, and M. Eichhorn, Opt. Lett. **39**, 6407 (2014).
15. Y. Sato, T. Taira, N. Pavel, and V. Lupei, Appl. Phys. Lett. **82**, 844–846 (2003).
16. M. Nadimi, T. Waritanant, and A. Major, Photonics Res. **5**, 346 (2017).
17. T. Waritanant and A. Major, Appl. Phys. B **122**, 135 (2016).
18. T. Waritanant and A. Major, Opt. Express **24**, 12851 (2016).
19. M. Nadimi, T. Waritanant, and A. Major, Laser Phys. Lett. **15**, 15001 (2018).
20. T. K. Kalkandjiev and M. A. Bursukova, Proc. SPIE **6994**, 69940B (2008).
21. D. P. O'Dwyer, K. E. Ballantine, C. F. Phelan, J. G. Lunney, and J. F. Donegan, Opt. Express **20**, 21119–21125 (2012).
22. C. McDonald, C. McDougall, E. Rafailov, and D. McGloin, Opt. Lett. **39**, 6691-6694 (2014).
23. A. Turpin, Y. Loiko, T. K. Kalkandjiev, and J. Mompart, Opt. Lett. **37**, 4197 (2012).
24. I. V. Mochalov, Opt. Eng. **36**, 1660 (1997).
25. P. Loiko, S. Manjooran, K. Yumashev, and A. Major, Appl. Opt. **56**, 2937–2945 (2017).
26. R. C. Talukder, M. Z. E. Halim, T. Waritanant, and A. Major, Opt. Lett. **41**, 3810 (2016).
27. M. Z. E. Halim, R. C. Talukder, T. Waritanant, and A. Major, Laser Phys. Lett. **13**, 105003 (2016).
28. R. Akbari, K. A. Fedorova, E. U. Rafailov, and A. Major Appl. Phys. B **123**, 123 (2017).
29. R. Akbari and A. Major, Appl. Opt. **56**, 8838–8844 (2017).
30. Y. V. Loiko, G. S. Sokolovskii, D. Carnegie, A. Turpin, J. Mompart, and E. U. Rafailov, Proc. SPIE **8960**, 89601Q (2014).
31. M. Nadimi, T. Waritanant, and A. Major, Laser Phys. Lett. **15**, 055002 (2018).
32. T. Waritanant and A. Major, Opt. Lett. **42**, 1149 (2017).

Full References

1. A. Turpin, Y. V. Loiko, T. K. Kalkandjiev, and J. Mompart, "Conical refraction: fundamentals and applications," Laser Photon. Rev. 10, 750–771 (2016).

2. A. M. Belsky and A. P. Khapalyuk, "Internal conical refraction of bounded light beams in biaxial crystals," Opt. Spectrosc. 44, 436 (1978).

3. A. M. Belsky and M. A. Stepanov, "Internal conical refraction of coherent light beams," Opt. Commun. 167, 1–5 (1999).

4. M. V. Berry, "Conical diffraction asymptotics: fine structure of Poggendorff rings and axial spike," J. Opt. A Pure Appl. Opt. 6, 289–300 (2004).

5. C. F. Phelan, K. E. Ballantine, P. R. Eastham, J. F. Donegan, and J. G. Lunney, "Conical diffraction of a Gaussian beam with a two crystal cascade," Opt. Express 20, 13201 (2012).

6. G. S. Sokolovskii, D. J. Carnegie, T. K. Kalkandjiev, and E. U. Rafailov, "Conical Refraction: New observations and a dual cone model," Opt. Express 21, 11125 (2013).

7. A. Turpin, Y. V. Loiko, T. K. Kalkandkiev, H. Tomizawa, and J. Mompart, "Super-Gaussian conical refraction beam," Opt. Lett. 39, 4349 (2014).

8. M. V. Berry, M. R. Jeffrey, and J. G. Lunney, "Conical diffraction: observations and theory," Proc. R. Soc. A Math. Phys. Eng. Sci. 462, 1629–1642 (2006).

9. J. Hellström, H. Henricsson, V. Pasiskevicius, U. Bünting, and D. Haussmann, "Polarization-tunable Yb:KGW laser based on internal conical refraction," Opt. Lett. 32, 2783 (2007).

10. A. Brenier, "Revealing modes from controlling an off-optical axis conical diffraction laser," Laser Phys. 27, 105001 (2017).

11. A. Abdolvand, K. G. Wilcox, T. K. Kalkandjiev, and E. U. Rafailov, "Conical refraction Nd:KGd(WO$_4$)$_2$ laser," Opt. Express 18, 2753 (2010).

12. A. Brenier, "Lasing with conical diffraction feature in the KGd(WO$_4$)$_2$:Nd biaxial crystal," Appl. Phys. B 122, 237 (2016).

13. K. G. Wilcox, A. Abdolvand, T. K. Kalkandjiev, and E. U. Rafailov, "Laser with simultaneous Gaussian and conical refraction outputs," Appl. Phys. B 99, 619–622 (2010).

14. R. Cattoor, I. Manek-Hönninger, D. Rytz, L. Canioni, and M. Eichhorn, "Laser action along and near the optic axis of a holmium-doped KY(WO$_4$)$_2$ crystal," Opt. Lett. 39, 6407 (2014).

15. Y. Sato, T. Taira, N. Pavel, and V. Lupei, "Laser operation with near quantum-defect slope efficiency in Nd:YVO$_4$ under direct pumping into the emitting level," Appl. Phys. Lett. 82, 844–846 (2003).

16. M. Nadimi, T. Waritanant, and A. Major, "High power and beam quality continuous-wave Nd:GdVO$_4$ laser in-band diode-pumped at 912 nm," Photonics Res. 5, 346 (2017).

17. T. Waritanant and A. Major, "Thermal lensing in Nd:YVO$_4$ laser with in-band pumping at 914 nm," Appl. Phys. B 122, 135 (2016).

18. T. Waritanant and A. Major, "High efficiency passively mode-locked Nd:YVO$_4$ laser with direct in-band pumping at 914 nm," Opt. Express 24, 12851 (2016).

19. M. Nadimi, T. Waritanant, and A. Major, "Passively mode-locked high power Nd:GdVO$_4$ laser with direct in-band pumping at 912 nm," Laser Phys. Lett. 15, 15001 (2018).

20. T. K. Kalkandjiev and M. A. Bursukova, "Conical refraction: an experimental introduction," Proc. SPIE 6994, Photon Management III, 69940B (2008).

21. D. P. O'Dwyer, K. E. Ballantine, C. F. Phelan, J. G. Lunney, and J. F. Donegan, "Optical trapping using cascade conical refraction of light," Opt. Express 20, 21119–21125 (2012).

22. C. McDonald, C. McDougall, E. Rafailov, and D. McGloin, "Characterising conical refraction optical tweezers," Opt. Lett. 39, 6691-6694 (2014).

23. A. Turpin, Y. Loiko, T. K. Kalkandjiev, and J. Mompart, "Free-space optical polarization demultiplexing and multiplexing by means of conical refraction," Opt. Lett. 37, 4197 (2012).

24. I. V. Mochalov, "Laser and nonlinear properties of the potassium gadolinium tungstate laser crystal KGd(WO$_4$)$_2$:Nd^{3+}-(KGW:Nd)," Opt. Eng. 36, 1660 (1997).

25. P. Loiko, S. Manjooran, K. Yumashev, and A. Major, "Polarization anisotropy of thermal lens in Yb:KY(WO$_4$)$_2$ laser crystal under high-power diode pumping," Appl. Opt. 56, 2937–2945 (2017).

26. R. C. Talukder, M. Z. Eibna Halim, T. Waritanant, and A. Major, "Multiwatt continuous wave Nd:KGW laser with hot-band diode pumping," Opt. Lett. 41, 3810 (2016).

27. M. Z. Eibna Halim, R. C. Talukder, T. Waritanant, and A. Major, "Passive mode locking of a Nd:KGW laser with hot-band diode pumping," Laser Phys. Lett. 13, 105003 (2016).

28. R. Akbari, K. A. Fedorova, E. U. Rafailov, and A. Major, "Diode-pumped ultrafast Yb:KGW laser with 56 fs pulses and multi-100 kW peak power based on SESAM and Kerr-lens mode locking," Appl. Phys. B 123, 123 (2017).

29. R. Akbari and A. Major, "High-power diode-pumped Kerr-lens mode-locked bulk Yb:KGW laser," Appl. Opt. 56, 8838–8844 (2017).

30. Y. V. Loiko, G. S. Sokolovskii, D. Carnegie, A. Turpin, J. Mompart, and E. U. Rafailov, "Laser beams with conical refraction patterns," Proc. SPIE 8960, p. 89601Q (2014).

31. M. Nadimi, T. Waritanant, and A. Major, "Discrete multi-wavelength tuning of a continuous wave diode-pumped Nd:GdVO$_4$ laser," Laser Phys. Lett. 15, 055002 (2018).

32. T. Waritanant and A. Major, "Diode-pumped Nd:YVO$_4$ laser with discrete multi-wavelength tunability and high efficiency," Opt. Lett. 42, 1149 (2017).